Environmental Science Advances

ROYAL SOCIETY OF CHEMISTRY

PAPER

View Article Online
View Journal | View Issue

Cite this: *Environ. Sci.: Adv.*, 2023, **2**, 484

An adsorption agent based on chitosan–zeolite composite: environmental and radioactive liquid waste remediation

Leandro Goulart de Araujo, †*[a] Vinicius Litrenta Medeiros,[b] Guilherme de Paula Guarnieri,[b] Danilo Antonio da Silva,[b] Tamires Watanabe,[a] Júlio Takehiro Marumo[a] and José Geraldo Nery[b]

In this article, we present a chitosan–zeolite composite, which was synthesized and used as an adsorbent material for caesium (Cs) removal from aqueous media and real liquid radioactive organic waste (LROW). The compound was characterized by X-ray diffraction, Fourier transform infrared spectroscopy, and scanning electron microscopy techniques. The physicochemical characterization indicates the production of a composite. Adsorption experiments were first performed using the prepared solutions contaminated with Cs using full factorial design with two variables of interest: initial Cs concentration (Cs_0) and adsorbent dosage (mg L^{-1}). The results indicated a high caesium removal rate with removal values above 93% and adsorption capacity of up to 10 mg g^{-1}. With the best experimental conditions according to our experimental domain, time was evaluated and equilibrium was reached in 180 min. Finally, the adsorbent material was tested as an adsorbent for Cs, Am, and U from LROW. When in contact with LORW, the removal rates (%) were 21.51 (^{137}Cs), 26.39 (^{241}Am), and 20.26 (U (total)). Although lower, this material indicated that it has the potential to be used for multi-elemental adsorption.

Received 29th June 2022
Accepted 27th January 2023

DOI: 10.1039/d2va00148a

rsc.li/esadvances

Environmental significance

Nuclear energy has been of great importance in the scenario of constant technological evolution and greater need for energy and is an attractive source due to the low emission of greenhouse gases. However, the radioactive waste generated is of concern and must be properly managed. The presence of radioactive caesium in liquid waste is of concern because it is a highly soluble and radiotoxic element. Therefore, the development of low-cost and efficient materials for the removal of this radionuclide and future immobilization is of great importance. Here we present a chitosan–zeolite composite capable of significantly removing this radionuclide and is also capable of removing other radionuclides such as uranium and americium in the presence of organic material.

Introduction

The nuclear accident that occurred in Fukushima in 2011 brought great concern to society about pollution in water resources caused by radionuclides.[1,2] Among the radionuclides formed during nuclear fission, there are the two radioactive isotopes of caesium, ^{134}Cs and ^{137}Cs.[3,4] In addition to being a concern in nuclear accidents, ^{137}Cs is routinely found in the radioactive waste from nuclear operations.[5,6] Furthermore, industries, hospitals, and research institutions produce wastewater contaminated with this radionuclide.[7,8]

Over time, the radioactivity of these isotopes will diminish to produce fewer radioactive elements. ^{137}Cs has a half-life of about 30 years and can endure for a significant period before evolving into a more stable element, ^{137}Ba with a half-life of only 2.6 min.[8,9] Radioactive caesium is the greatest challenge amid the radionuclides not only because of its long half-life and high solubility but also due to its high specific radioactivity and capability to move toward living organisms. Consequently, it can harm water resources, affecting plants and animals such as potassium, a crucial element in the environment.[10]

As regards the dangers related to human beings, ^{137}Cs is of great concern mainly due to cancer in organs such as the pancreas,[11] and cervical[12] and thyroid glands.[13] The potent radiation of this nuclide is also able to destroy the biological cells of several organisms, causing failures of their functions and consequently critical genetic-related diseases.[14]

Therefore, effective treatments for the removal of ^{137}Cs from the environment are essential to guarantee the safety of living beings. Among a multitude of methods that have been

[a]*Nuclear and Energy Research Institute (IPEN), Av. Prof. Lineu Prestes 2242, São Paulo, SP, 05508-000, Brazil. E-mail: lgoulart@alumni.usp*

[b]*Department of Physics, Institute of Bioscience, Letters and Exact Sciences, São Paulo State University (UNESP), Campus of São José do Rio Preto, SP, 15054-000, Brazil*

† Present address: Institut Jean Lamour, CNRS UMR7198, Université de Lorraine, Ecole Nationale Supérieure des Technologies et Industries du Bois (ENSTIB), 27 Rue Philippe Séguin, BP 1041, 88051 Epinal Cedex 9, France.

employed to remove ^{137}Cs from radioactive wastewater and contaminated waters, the adsorption technique stands out.[15] The reason is that this technique is simple, efficient, and can be applied to treat great volumes of contaminated water with low concentrations of nuclides.[16]

Some examples of natural adsorption agents used for ^{137}Cs remediation are zeolites, aluminium molybdophosphate, ammonium 12-molybdophosphate (AMP), and other natural agents.[14] Beyond the natural agents, synthetic agents are also used for ^{137}Cs remediations, and among these agents, the composites stand out.[14,17]

Composites are mixed materials composed of two or more different sources, producing new materials with different properties to expand or improve the possible applications when compared to separated matrices.[18] Two materials that are interesting for composite synthesis by ion remediation are chitosan and zeolites.

Chitosan is a chitin derivative polysaccharide with 2-amino-2-desoxy-D-glicopiranose as a monomeric unit, with binding between these units.[19–21] Due to the chemical and structure properties of chitosan, this biopolymer can be used as an adsorption agent, hemostatic agent, cross-linking agent, drug delivery, and other applications.[22,23]

The main mechanism related to the adsorbent features of chitosan-based adsorbents is due to its amino and hydroxyl groups, in addition to having multiple chelation sites. These characteristics allow the attraction between the metal ions by the coordination bond or by ion exchange.[24]

Zeolites are defined as polycrystalline aluminosilicates. These crystals are formed by silica and aluminium tetrahedrons, when the silica or aluminium atoms bind with four oxygen atoms. Zeolites show a periodic arrangement of cages and channels of molecular dimensions.[25] Due to their structural and chemical properties, zeolites are reported in a large type of applications, such as catalysis, molecular sieves, hemostatic agents, and adsorption agents.[26,27] The presence of open pores, also called cavities, is in an ab-ordered arrangement. The three main reasons for using zeolites as adsorbent materials are related to their remarkable cation-exchange capability, their molecular sieve characteristics, and the arrangements that can be made for each application of interest.[28] The net negative charge of the aluminium tetrahedra unit is secured by interchangeable cations, *i.e.*, Ca^{2+}, K^{+}, and Na^{+}, which can be substituted by heavy metals such as caesium.[29] According to Khandaker *et al.* (2020),[29] the inorganic ion exchangers are unrivalled when compared to other ion exchangers because of their higher radiation stability.

Chitosan–zeolite composites are reported as ion adsorptions agents, due to the properties of zeolite,[30] and chitosan.[31] In the literature it is reported that these materials are formed from different types of zeolites, such as clinoptilolite, ZSM-5, BEA, NaY, and other types of zeolite,[32] and these composites are used for remediation of different ions, such as Cu^{2+}, Co^{2+}, Ni^{2+}, UO_2^{2+}, Th^{2+}, F^{-}, VO^{2+}, and VO_3.[32–36] Nevertheless, systematic studies with chitosan–zeolite composites have not been reported for the Na–X zeolite as the zeolitic matrix for radioactive ions removal for water media, especially caesium.

As found from the literature, adsorption is influenced by many physicochemical factors such as pH, initial pollutant concentrations, and adsorbent dosage,[37] and their interactions are so complex that the generation of empirical models that do not take into account their influence, usually do not provide sufficient information and may yield unsatisfactory predictions. In fact, most studies rely on assessing the effects involved in the adsorption process by employing the traditional "one-factor-at-a-time" (OFAT) approach to experimentation. According to Jasper *et al.* (2021),[38] the drawbacks of OFAT are that they are time-consuming and tedious. Another point of concern is that less information is obtained, hampering the understanding of the process. Furthermore, the OFAT models are less reproducible, particularly when other values for the experimental conditions in the range studied are conducted.

According to Montgomery *et al.*,[39] the application of factorial experimental design is an adequate choice for minimizing these difficulties since all the parameters of interest are optimized. Moreover, the factorial experimental design requires (i) a few experiments; (ii) providing more complete mathematical models; (iii) the use of statistics to enable the search for more efficient experimental domains.

In this study, a chitosan–zeolite composite was synthesized and tested as an adsorption material. A full two-level factorial design was applied to evaluate the effect of two experimental variables: the solution's initial concentration and adsorbent dosage, besides their interactions on the removal percentage and adsorption capacity of this new composite on caesium adsorption. To the best of our knowledge, the influence of these variables on caesium removal through this composite has not been previously investigated by experimental design and response surface methodologies. The empirical equations generated by the experimental design examine not only each variable but also their interactions, providing more useful mathematical models. Furthermore, the composite was also tested as a biosorbent of caesium, americium, and uranium in real organic radioactive waste from a nuclear reactor.

Methods

Synthesis of zeolites matrix

The zeolite matrix (FAU framework) was synthesized by hydrothermal crystallization following the procedure described below: the precursor gel was prepared by mixing freshly prepared aluminate and silicate solutions at a molar ratio of $5.5Na_2O : 1.0Al_2O_3 : 4.0SiO_2 : 190H_2O$. In a typical synthesis, sodium hydroxide solution (5.34 g of NaOH/50 mL of H_2O) was freshly prepared, followed by the addition of 2.42 g of sodium aluminate ($NaAlO_2$), with stirring for 15 min at room temperature. Fumed silica (SiO_2, 3.43 g) was then added to the solution with stirring until a homogeneous gel was obtained. The gel was immediately transferred to a static reactor (Parr Instruments Co., USA) at 90 °C for 4 days.

Synthesis of chitosan–zeolite composite

The composite was synthesized according to the procedure described by Ngah *et al.* but with modifications.[40] The reactants

and their respective amounts for a typical synthesis are 2.0 g of synthesized zeolite, 2.0 g of commercial medium molecular weight chitosan (Sigma – Aldrich) with 75–85% deacetylation degree and 190–310 kDa, 3.9 mL of glacial acetic acid (Merk), 3.0 g of sodium hydroxide (Sigma – Aldrich), and 376.1 mL of distilled water.

The synthesis was performed according to the following procedure: firstly, 130 mL of 3% acetic acid solution (pH around 3) and 250 mL of 0.3 M sodium hydroxide solution (pH around 12) were prepared. Zeolite and chitosan were added to 80 mL of the acetic acid solution and then vigorously stirred for 2 h. After this, 50 mL of the same acetic acid solution was also added and then stirred for 1 h. Subsequently, this mixture was dripped in the sodium hydroxide solution in a precipitation bath. When dripping was complete, the solution was stirred for 3 h. The composite was filtered (pH of the liquid phase around 11) and was washed with distilled water until neutralization. The material was dried in the oven at 80 °C, overnight.

Physicochemical characterization

The XRD patterns of the synthesized materials were collected using a Rigaku Miniflex II X-ray Diffractometer, operating at 15 mA and 30 kV, with a Cu Kα radiation ($\lambda = 1.5418$ Å) and a nickel filter. The patterns were obtained in the 2θ range from 3° to 50°, at a scan rate of 2° (2θ) min^{-1}. The FT-IR analyses were performed using a Shimadzu IRTracer-100 spectrometer. The samples were prepared using the KBr method. The spectra were collected in the wavenumber range from 400 cm^{-1} to 4000 cm^{-1}.

The scanning electron microscopy (SEM) images were recorded at the Structural Characterization Laboratory of Materials Engineering Department of the Federal University of São Carlos (LCE-DEMa-UFSCar) using an FEI Inspect S 50 microscope. The images were obtained with an electron beam voltage of 25 kV.

Adsorption experiments

All solutions were prepared with analytical-grade chemicals and distilled water. The contaminated solution was prepared with cesium chloride (Honeywell Fluka, USA), and set with initial ^{133}Cs concentrations of 10 and 50 mg L^{-1} at the natural pH of these solutions (3). ^{137}Cs (radioactive) solutions were prepared from a stock (Amersham, England) and used as a tracer. More information will be given in the "Gamma spectrometry" section. The adsorbent was added in 50 mL polypropylene vials with 10 mL of solution with a dosage of 5 or 15 g L^{-1}. The flasks were then mixed on an orbital shaker at 130 rpm under a controlled temperature (25 ± 2 °C). The samples were continuously agitated for a contact time of 24 h. Then, each tube was centrifuged for 30 min at 3600 rpm to separate the supernatant. All liquids were then analysed. The optimum conditions were selected based on the adsorbent dose and initial caesium concentration. The extraction efficiency, R (%), was determined using eqn (1), while the adsorption capacity (q, mg g^{-1}) of the adsorbent was calculated using eqn (2):

$$R\ (\%) = 100 \times \left[\frac{(C_0 - C_t)}{C_0}\right] \quad (1)$$

$$q_t = (C_0 - C_t)\frac{V}{m} \quad (2)$$

where R is the extraction efficiency or the retention percentage; C_0 and C_t are the concentrations of the adsorbate in the initial solution and at any time t, respectively (mg L^{-1}); q_t is the adsorbed amount of adsorbate per gram of the adsorbent at time t, V is the volume of the added adsorbate solution (L) and m is the amount of the adsorbent used (g).

Two-level factorial design

Caesium removal by the zeolite–chitosan composite in batch experiments may rely on many variables, including adsorbent dosage (A) and initial adsorbate concentration (B). A complete factorial design was developed by considering these two factors.[41] The full 2^2 factorial design requires 4 experiments, which were performed in duplicate, totalling 8 experiments. The coded and real values of each variable are shown in Table 1.

Both independent variables are numeric, favouring additional variations at any suitable numerical level. RStudio was the software of choice for evaluating the effects of this experimental design.[42] The R package "pid" was used for the analysis.[43] Analysis of the variance and data obtained were used to evaluate the proposed system. For a better understanding of the obtained results, we used Pareto and contour graphs.

Kinetics

After determining the best experimental conditions according to our experimental design with regard to adsorption capacity and caesium removal percentage, batch sorption experiments were performed to assess the effect of the contact time. The same experimental procedures as those described in "Adsorption experiments" were conducted. The experimental conditions used were those from experimental run 3 (Table 1). The vials containing the solutions contaminated with caesium were

Table 1 Coded and real values for dosage (A, g L^{-1}) and $[^{133}Cs]_0$ (B, mg L^{-1})

Experimental run (standard order)	X_A (coded)	X_B (coded)	A (real)	B (real)
1	−1	−1	5	10
2	+1	−1	15	10
3	−1	+1	5	50
4	+1	+1	15	50

kept in contact during different time intervals: 0, 5, 15, 30, 60, 120, 180, and 240. Again, the experiments were carried out in duplicate.

Kinetic adsorption modelling was used to mathematically describe the adsorption of caesium onto the chitosan–zeolite composites. Two non-linear kinetic models were applied to our experimental data, the pseudo-first order (PFO)[44,45] and the pseudo-second order (PSO)[46] The kinetic equations used were:

$$q_t = q_e\,(1 - \exp^{(-k_1 t)}) \quad (3)$$

$$q_t = \frac{k_2 q_e^2 t}{1 + k_2 q_e t} \quad (4)$$

where t is the contact time (min), q_t is the amount of the adsorbate adsorbed at the time (mg g^{-1}), q_e is the equilibrium adsorption capacity (mg g^{-1}), k_1 is the pseudo-first order rate constant (min^{-1}) and k_2 is the pseudo-second order rate constant (g mg^{-1} min^{-1}).

Gamma spectrometry

A high-purity coaxial detector (HPGe) gamma spectrometer (Falcon 5000, Canberra) was used to identify and measure ^{137}Cs and ^{241}Am. Activities due to the background measurements were removed for correct analysis. The "*In Situ* Object Counting Systems" (ISOCS) software was used to generate efficiency curves from the geometry supplied by the user and then supplied to the Canberra Genie 2000 software, which generated the counting spectra. Counting was performed for 600–3600 s depending on the activity of the samples. From the library of radionuclides, the specific ^{137}Cs and ^{241}Am gamma energy lines were examined, and their activity was measured. The photopeaks of 661.65 keV and 59.54 keV were used for measuring ^{137}Cs and ^{241}Am activity concentrations, respectively. A radioactive standard containing only ^{137}Cs in water was used and diluted to the desired activity concentrations. The initial concentration of ^{137}Cs activity was 28.5 Bq mL^{-1} of the solution. The tracer removal percentage (^{137}Cs) is the same as ^{133}Cs, so the results were obtained in the percentage removal activity and converted to mg L^{-1} after ^{133}Cs removal.

Measurement of uranium (U) by ICP-OES

Inductively coupled plasma optical emission spectroscopy (ICP-OES) instrument, model Optima 7000DV (PerkinElmer, USA) was used to measure the total U concentration. Calibration solutions were prepared by dilution of the certified uranium solution (Johnson Matthey Company, UK). The wavelength (λ) used in the determination of uranium was 424.167 nm, and the results are expressed as the average of triplicate measurements.

Adsorption tests with real radioactive waste

The liquid radioactive waste employed is composed of water, ethyl acetate (196 mg L^{-1}), tributyl phosphate (227 mg L^{-1}), and many radionuclides, especially ^{137}Cs, ^{241}Am, and U (total). The pH value was about 3 because of the considerable amount of nitric acid in the liquid waste. The concentrations of these radionuclides in the selected liquid waste are ^{137}Cs = 7.27 × 10^{-6} mg L^{-1}, ^{241}Am = 1.78 × 10^{-4} mg L^{-1}, U (total) = 2.23 × 10^{2} mg L^{-1}. These wastes were generated in research and development activities in the IPEN's IEA-R1 nuclear reactor. The selected dosage used for these experiments was 5 g L^{-1}.

Results and discussion

Fig. 1 shows the XRD patterns of the composite (blue line), and its precursors materials (zeolite is black and chitosan is red). The composite pattern has characteristic peaks of its precursor materials, but the intensities of these peaks are lower than those from the original materials. Furthermore, some characteristic peaks of zeolites disappear in the composite (blue arrows). These results indicate that the material has the structural characteristics of the original ones. Moreover, data indicate the interaction between the silanol groups on the zeolite surface with amine groups of chitosan, highlighting the formation of the zeolite–chitosan composite.[47]

Fig. 2 shows the FT-IR spectra of the materials. The composite spectrum has the following absorption bands. The band at 3440 cm^{-1} is due to the stretching of the hydroxyl group, the band at 2927 cm^{-1} refers to the stretching of the C–H aliphatic group, the band in 2880 cm^{-1} is due to the stretching of the C–H group in bound O–CH–O, the band in 1651 cm^{-1} refers to NH_2 group flexion, the band in 1557 cm^{-1} is assigned to NH_3^+ vibrational deformation, the band in 1379 cm^{-1} refers to flexion of bound C–H, the band in 1311 cm^{-1} is due to C–N bound stretching, the band in 1006 cm^{-1} is assigned to Si–O stretching, the band in 700 cm^{-1} is due to asymmetric stretching of bound Si–O, the band in 599 cm^{-1} refers to Al–O–Si stretching, and the band in 455 cm^{-1} is assigned to the flexion of the bound Si–O.[40,48]

The changes of transmittance values in the composite spectrum in comparison with the original material spectra in the absorptions band were assigned to the N–H bound in the chitosan spectrum and to the Si–O in the zeolite spectrum. These changes underline that the composite is formed by the interaction between amine groups of chitosan and silanol groups presents in zeolite surface, also previously observed in

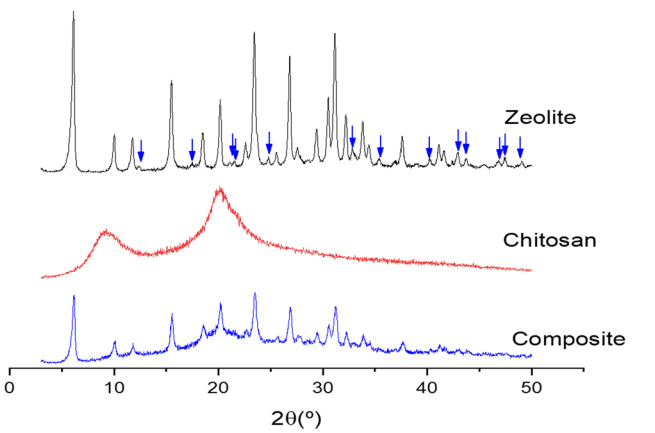

Fig. 1 XRD patterns.

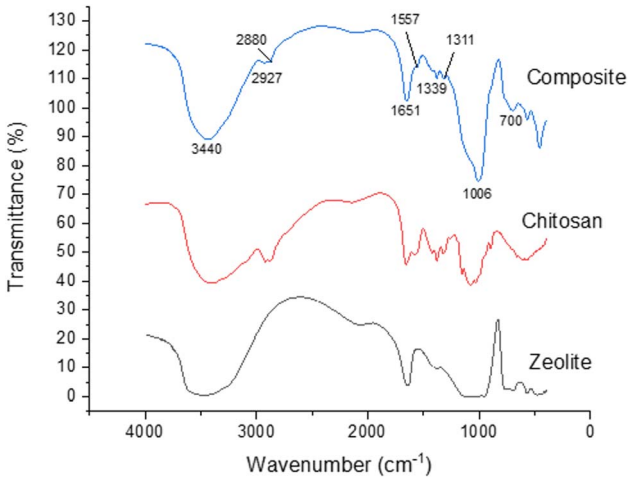

Fig. 2 FT-IR spectra.

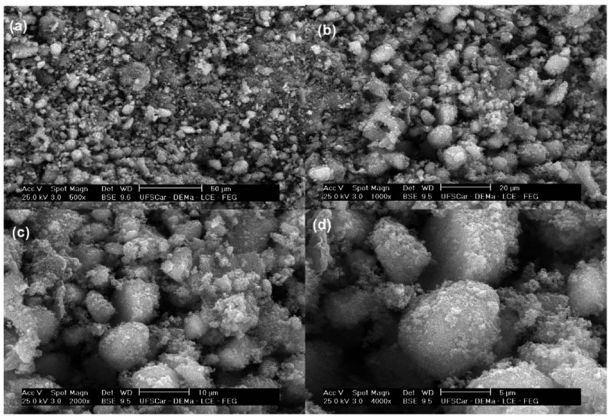

Fig. 3 SEM images of the composite. (a) Mag 500×, (b) mag 1000×, (c) mag 2000×, (d) mag 4000×.

XRD data. The XRD and FT-IR data suggest the composite formation.

Fig. 3 shows SEM images of the chitosan–zeolite composite. Typically, the material presents an irregular morphology and plenty of debris on the material surface.

Table 2 lists the adsorption results of caesium by the chitosan–zeolite composite. Caesium removal values were high, above 93.80%. Furthermore, the adsorption capacity of the synthesized composite (q, Y_2) was attractive, reaching values close to 10 mg g^{-1}. When compared to the literature, the adsorption capacities were similar to other adsorbents of caesium.[49] Employing raw wood charcoal and functionalized wood charcoal with nitric acid, resulted in capacities of 2.76 and 9.14 mg g^{-1}, respectively. Note that adsorption capacity is directly related to the dosage of the adsorbent. This means that changes in the adsorbent mass or liquid volume could influence the final material capacity. As an example, Khandaker *et al.* (2020)[29] found three different adsorption capacities, 1.995 mg g^{-1} ($[Cs]_0 = 20$ mg L^{-1}), 9.457 mg g^{-1} ($[Cs]_0 = 100$ mg L^{-1}), and 27.818 mg g^{-1} ($[Cs]_0 = 400$ mg L^{-1}). In this context, the chitosan–zeolite composite has potential compared to other materials. Furthermore, optimizations with lower amounts of adsorbent or greater volume of the solution may promote a boost in terms of capacity. Since the percentage of removals was high, variations in these independent variables are expected to significantly increase its value. Therefore, this material is promising for the removal of caesium-contaminated solutions.

Table 3 shows a summary of the empirical model for Y_2. For Y_1, since the values were very close, only the linear coefficient was statistically significant. Fig. 4 shows the Pareto chart and the contour plot for Y_2.

As seen in Table 3, the empirical mathematical model is:

$$Y_2 = 3.83 - 1.88A + 2.54B - 1.23AB \quad (5)$$

In relation to Y_1, none of the parameters presented statistically significant effects on the result, being only the intercept enough to predict the data. The reason is that the values were very close, preventing any interpretation regarding different values for the assessed parameters. In relation to Y_2, B ($[^{133}Cs]_0$) plays the major role and has a positive effect on the system's

Table 3 Summary of the equation of the linear model of adsorption capacity of the zeolite–chitosan composite. Standard error = 0.38 (Y_1) and 0.02 (Y_2). Stepwise regression was used to give the most statistically significant improvement in the fit with chi-squared distribution of $k = 3.841450$ (probability = 0.95, degrees of freedom = 1)

The adsorption capacity of the synthesis composite (Y_2)			
Coefficients	Estimate	t value	Pr (>|t|)
(Linear coefficient)	3.83012	151.21	1.15×10^{-8}
A	−1.87805	−74.14	1.98×10^{-7}
B	2.53646	100.14	5.96×10^{-8}
$A:B$	−1.23372	−48.71	1.06×10^{-6}
R^2	0.9998		

Table 2 Actual values for dosages (A, g L^{-1}) and $[^{133}Cs]_0$ (B, mg L^{-1}). Y_1 is the percent removal and Y_2 is the adsorption capacity of the zeolite–chitosan compound

Experimental run (standard order)	Dosage (A, real, g L^{-1})	$[^{133}Cs]_0$ (B, real, mg L^{-1})	Y_1 (%)	Y_2 (mg g^{-1})
1	5	10	96.90 ± 1.60	1.94 ± 0.03
2	15	10	97.40 ± 0.30	0.65 ± <0.01
3	5	50	94.78 ± 1.39	9.48 ± 0.14
4	15	50	97.64 ± 0.34	3.25 ± 0.01

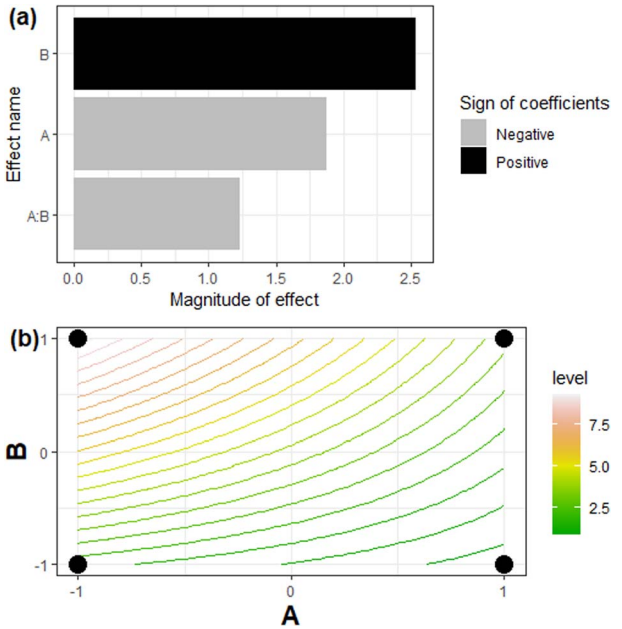

Fig. 4 (a) Pareto plots from the parameters calculated by the mathematical model for Y_2 (adsorption capacity of the composite, mg g^{-1}); (b) contour plot of actual values for dosage (A, g L^{-1}) and $[^{133}Cs]_0$ (B, mg L^{-1}). Levels are predictions for Y_2 (mg g^{-1}).

adsorption capacity, while A (dosage) negatively influences it (Fig. 4(a)). The interaction effect between these parameters is less relevant for Y_2 and has a negative influence. In other words, increasing the initial concentration of caesium benefits the maximization of this dependent variable.

On the other hand, the dosage must decrease to reach higher q values. Fig. 4(b) details the models' predictions for variations in the Y_2 values, with the line curvatures, indicating the important $A:B$ interaction term for these experiments. pH increased from 3 (prepared solution) to 6.5–7.2, indicating a similar final pH regardless of the experimental conditions used.

The selection of the best values for each of the parameters depends on the strategy to reach a desirable final caesium concentration or to search for the maximum capacity of the adsorbent (q_{max}). Since this work proposes the use of a novel material to be used as an adsorbent for caesium-contaminated solutions, we focused on the response of adsorption capacity. In this case, the experimental conditions observed in experimental run no. 3 reached the highest values for this response. Because of that, kinetics was assessed by several contact times until equilibrium was reached. Fig. 5 shows the kinetics of caesium adsorption by the composite over time.

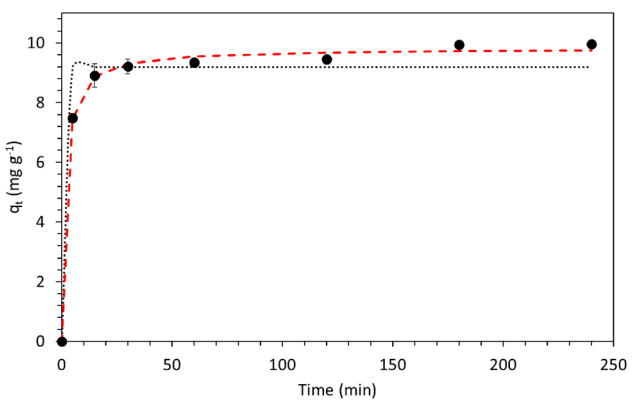

Fig. 5 Kinetics for caesium adsorption by the composite over time.

As expected, the adsorption of caesium increased over time until equilibrium was reached. The equilibrium time was reached after 180 min. Equilibrium time for this material was faster than that found on raw wood charcoal (240 min) but slower than that found on the functionalized wood charcoal (60 min) with nitric acid.[49,50] For the modified cellulosic charcoal, an equilibrium time of 300 min for the same concentration was employed (50 mg L^{-1}) but it achieved 100% of removal. In the first 5 min, the pH increased from 3 to 6, and then slightly to 7 after 30 min, remaining stable during the observed 240 min, indicating that the process was stable. Table 4 shows the efficiency of the Cs^+ removal achieved by the composite prepared in this study in comparison with other materials reported in the literature. It is observed in Table 4 that the material studied in this work removed more Cs^+, in percentage terms, in comparison with other works. In terms of the adsorption capacity, the composite reaches values close to some works present in this table, in some cases, such as that by Nakamura *et al.*[45] and Eljamal *et al.*,[51] who used magnetic zeolites to prepare the composites. It indicates the potential of this composite for caesium removal.

Chitosan–zeolite composites have also been employed to remediate aqueous solutions contaminated by metallic ions, Cu^{2+};[52,53] Cd^{2+};[54] Cr^{6+};[55,56] As^{5+};[57] and other ions.[32,58] The maximum adsorption capacity, in some cases, is higher than the capacity observed in this work, such as the work reported by Ngah *et al.*,[53] in which a chitosan–LTA zeolite composite was used for copper removal, reaching maximum adsorption of 51.32 mg g^{-1}. Pang *et al.*[56] assessed a chitosan–LTA zeolite composite for chromium(VI) removal and found a maximum adsorption capacity of 70 mg g^{-1}. In the case of work reported by Zhang *et al.*,[54] a chitosan–LTL zeolite composite was used for cadmium removal and provided a maximum adsorption capacity of 102.15 mg g^{-1}. Han *et al.*[57] employed a chitosan–FAU zeolite composite for arsenic removal and reached a maximum adsorption capacity of 63.23 mg g^{-1}. One reason for the difference between the maximum adsorption capacity values is the different nature between these cations when compared with caesium. Caesium is an alkaline metal, and the cations shown above are transition metals. Caesium has a higher atomic radius than copper, cadmium, and chromium. These differences can be the reason for the variations observed between these adsorption capacity values. Furthermore, the literature indicates that some cations, like Pb^{2+}, Cu^{2+}, and Cd^{2+} have more affinity for chitosan–zeolite composite than other cations.[32,59,60] However, the results obtained in this work show the large potential of the composite as caesium remediation agent, mainly due to the removal rate, in percentage terms.

Table 4 Comparison of our results for the removal of Cs with other works reported. D = dosage, T = time, R = removal, q_{exp} = experimental adsorption capacity

Adsorbent material	$[Cs]_0$ (mg L^{-1})	D (g L^{-1})	T (h)	R (%)	q_{exp} (mg g^{-1})	Ref.
NaX–chitosan	10	5	24	97	1.9	Our work
NaX–chitosan	50	5	24	96	9.5	Our work
Iron nanoparticles–zeolite (nZVI–Z)	50	10	6	91	170.2	51
	100	10	6	96	277.4	
	150	10	6	96	258.6	
	200	10	6	95	223.8	
Iron nanoparticles–zeolite (nFe/Cu–Z)	50	10	2	59	3.0	51
	100	10	2	65	6.5	
	150	10	2	66	9.9	
	200	10	2	64	12.9	
Calix [4] arene–mordenite (NaNCl)	700	10	2	70	3.5	63
Calix [4] arene–mordenite (NaNCh)	700	10	2	74	7.4	
Calix [4] arene–mordenite (NaNM)	700	10	2	71	10.6	
Calix [4] arene–mordenite (NaSM)	700	10	2	65	13.1	
Iron oxide–NaA	0.01 N[a]	10	2	81	109.1	44
Zeolite	100	3.17	1.5	90	88.4	45
Fe10.7-MZC	100	3.17	1.5	>90	91.1	
Polymer/magnetite/zeolite (PMZ)	100	3.17	1.5	90	87.1	
Magnetite	100	3.17	1.5	<10	6.7	
Bn–CTS beads	200	5	20	93	36.5	64

[a] The cited paper employed normality units.

Both pseudo-first-order and pseudo-second-order were used to predict adsorption by using experimental data. The parameters obtained in the kinetic models are listed in Table 5.

Clearly, the pseudo-second-order model highlighted a much higher fit, with an R^2 value of 0.98. This is an indication that the rate-limiting step was probably due to the chemisorption of caesium from the solution onto the composite, besides indicating that this material is abundant with active sites[61,62] This corroborates with the mechanism of caesium removal seen in the literature, which found that the pseudo-second-order model as the most appropriate mechanism. Some examples involve the use of synthetic zeolites from bioslag.[29]

To check for the applicability of this material in removing caesium from a complex radioactive waste solution, experiments were performed with LORW. In terms of the percentage removal, we found 21.51 ± 0.29% for ^{137}Cs, 26.39 ± 8.20% for ^{241}Am, and 20.26 ± 0.32% for U (total). As regards the adsorption capacity, we found $3.11 \times 10^{-7} \pm 4.24 \times 10^{-9}$ mg g^{-1} for ^{137}Cs, $1.01 \times 10^{-5} \pm 3.12 \times 10^{-6}$ mg g^{-1} for ^{241}Am, and 9.02 ± 1.41×10^{-1} mg g^{-1} for U (total). As expected, caesium removal was much lower when the material was in contact with LORW.

Table 5 Parameters of the calculated kinetics

Nonlinear models	Parameters	Values
Pseudo-first-order	q_{eq} (mg g^{-1})	9.19
	K_1 (min^{-1})	16.25
	R^2	0.6842
Pseudo-second-order	q_{eq} (mg g^{-1})	9.80
	K_2 (g mg^{-1} min^{-1})	0.06
	R^2	0.9854

Some possible reasons are (1) the different order of magnitude concerning the concentration of this element in the synthetic and LORW solutions; (2) the presence of the organic content, which may impair the adsorption capacity of the materials; (3) the competition of the elements by the adsorption sites of the adsorbent must also be considered.

There are few works in the literature in which the biosorption of caesium, americium, and uranium has been evaluated, particularly in the presence of other radionuclides at lower concentrations, organic content, and low pH. Ferreira *et al.*[5] employed rice and coffee husks for the biosorption of these radionuclides also in real radioactive organic waste. The authors found a lower adsorption capacity (~8-fold) for ^{137}Cs (4.66×10^{-8} mg g^{-1}) but higher capacities (~14-fold) for U (total) (1.96 mg g^{-1}) and ^{241}Am (~4-fold) (3.94×10^{-5} mg g^{-1}).[65] They used raw and activated coconut fibre to treat a similar waste. In comparison with the NaX–chitosan, regarding ^{137}Cs, these materials presented much lower adsorption capacities: 4.47×10^{-8} mg g^{-1} (raw) and 3.77×10^{-8} mg g^{-1} (activated). For U (total), the raw coconut fibre presented a lower capacity (0.66 mg g^{-1}) and the activated fibre presented a higher capacity (0.90 mg g^{-1}). For ^{241}Am, these materials presented higher adsorption capacities, with 4.63×10^{-5} mg g^{-1} (raw) and 7.34×10^{-5} mg g^{-1} (activated).

Watanabe *et al.*[37] used hydroxyapatite and bone meal to treat uranium (U (total)) in a LORW. In terms of this radionuclide, the authors found greater adsorption capacity, with 22 mg g^{-1} and R (%) = 99.34%. Nevertheless, the adsorption of ^{137}Cs and ^{241}Am were not investigated. Vieira *et al.*[66] employed the macrophyte *Lemna* sp. to treat U (total) in another LORW. They found an adsorption capacity of 2.20 mg g^{-1}, three times higher

than that obtained with NaX–chitosan (0.90 mg g^{-1}). Araujo *et al.*[67] employed the macrophyte *Azolla* sp. to treat U (total) present in LORW and also found a higher adsorption capacity of 2.69 mg g^{-1}. It is worth mentioning that the focus of their work was on uranium treatment, whereas, in this work, the focus was on caesium treatment. Note that these differences may be due to the different characteristics of the LORW solutions used. For instance, the concentration of these radionuclides in this work are different from those found by Ferreira *et al.*,[5] especially americium (10-fold lower in our work) and uranium (2-fold higher in our work). Compared to published work on caesium removal, NaX–chitosan shows itself to be an attractive material for this element.

According to Watanabe *et al.*,[37] three main mechanisms may occur in the removal of elements such as uranium when in contact with an adsorbent. These mechanisms are adsorption, dissolution–precipitation, and ion exchange. Although the process is considered complex, pH is considered to be an adequate method to understand which are the main mechanisms involved in this type of process.

All experiments indicated an increase in pH from 3 to 6–7 (Fig. 6), which suggests that the dissolution–precipitation mechanism was potentially the main process during the experimental runs. This could occur from the partial dissolution of the adsorbent depending on pH conditions, such as acidic ones in both synthetic and LORW solutions. Ngah *et al.*[53] used a chitosan–zeolite composite in the removal of Cu(II) from aqueous solutions and found that the dissolution of chitosan occurs in low pH, which may have reacted with caesium and other compounds, forming new phases. The increased pH may have aided the adsorption of caesium, americium, and uranium by decreasing the competition between H_3O^+ that can occur under acidic conditions as well as decreasing electrostatic repulsion between ions such as Cs and H^+.[53] Furthermore, the equilibrium reached in terms of pH in less than 1 hour is an indication that the adsorption process was stable.

In terms of the adsorption capacity of NaX–chitosan, we found $q_{eq,U(total)} > q_{eq,Am\text{-}241} > q_{eq,Cs\text{-}137}$. The main reasons for such results are due to the much higher concentration of U (total), followed by ^{241}Am, and then ^{137}Cs. However, the removal percentages of these nuclides were: $R_{Am\text{-}241} > R_{Cs\text{-}137} > R_{U(total)}$, highlighting that even with the differences in terms of concentration, the percentage of caesium removal is comparatively high. LORW is complex due to its multicomponent nature, which makes it difficult to fully understand the process. However, some reasonable assumptions can be made that explain the reasons why NaX–chitosan has a high affinity for this element. According to Kexin *et al.*,[64] chitosan composites are able to adsorb Cs(I) prior to H^+, given the electrostatic interactions between this ion and N atoms. Furthermore, the presence of U (total) and ^{241}Am may not have significantly interfered with the adsorption of ^{137}Cs. El-Din *et al.*[68] employed ordered mesoporous monetite to decontaminate radioactive caesium in synthetic solutions. They evaluated the effect of competing species in four different groups. The so-called group IV (Cs(I), Cu(II), La(III), Zr(IV), U(VI), and Th(IV)), the only group containing elements with valences greater than three, highlighted the highest caesium removal, with 98.6%. On the other hand, the presence of caesium may have hindered the removal of uranium and americium, although these elements have much higher concentrations because monovalent ions can more easily occupy a hydrated state, given their higher hydration energy.[68] Finally, the pore size of the NaX–chitosan is 7.4 Å (circular), allowing the entry of the three nuclides, which have the ionic radius of 3.0 Å (Cs(I)), 2.00 Å (Am(III)), and 1.75 Å (U(VI)).

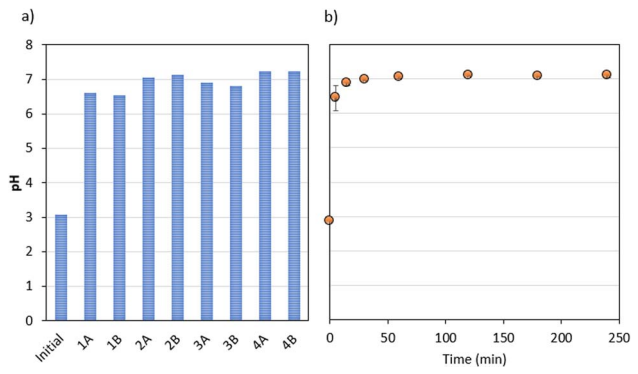

Fig. 6 Temporal profiles of pH during the experiments with (a) synthetic solutions (see Table 1 for the experimental conditions); (b) liquid radioactive organic waste.

Conclusion

A new chitosan–zeolite composite based on zeolite Na–X was prepared and fully characterized by XRD, FT-IR, and SEM. Experimental data obtained in this study have shown that the composite provided a feasible alternative in the treatment of aqueous solutions containing Cs with removal rates superior to 94%, and adsorption capacities of Cs^+ close to 10 mg g^{-1}. The zeolite–chitosan composite also has the potential of being used for the treatment of complex solutions such as the LORW since removals superior to 20% for ^{137}Cs, ^{241}Am, and U (total) were obtained.

Author contributions

Leandro Goulart de Araujo: conceptualization, data curation, formal analysis, investigation, methodology, and writing – original draft; Vinicius Litrenta Medeiros: conceptualization, data curation, formal analysis, investigation, methodology, resources, and writing – original draft; Guilherme de Paula Guarnieri: investigation; Danilo Antonio da Silva: investigation; Tamires Watanabe: investigation; Júlio Takehiro Marumo: data curation, investigation, and methodology; and José Geraldo Nery: conceptualization, formal analysis, founding acquisition, project administration, writing – original draft, and writing – review and editing.

Conflicts of interest

There are no conflicts to declare.

Acknowledgements

This work was supported by National Council for Scientific and Technology Development (CNPq) (grant # 131642/2018-9), and by the Nuclear and Energy Research Institute (IPEN). The authors thank the Laboratory of Structural Characterization (LCE/DEMa/UFSCar) for the general facilities.

References

1 B. Hu, Y. Ma and N. Wang, A novel water pollution monitoring and treatment agent: Ag doped carbon nanoparticles for sensing dichromate, morphological analysis of Cr and sterilization, *Microchem. J.*, 2020, **157**, 104855.

2 J. Wang, S. Zhuang and Y. Liu, Metal hexacyanoferrates-based adsorbents for cesium removal, *Coord. Chem. Rev.*, 2018, **374**, 430–438.

3 O. Falyouna, O. Eljamal, I. Maamoun, A. Tahara and Y. Sugihara, Magnetic zeolite synthesis for efficient removal of cesium in a lab-scale continuous treatment system, *J. Colloid Interface Sci.*, 2020, **571**, 66–79.

4 J. Wang and S. Zhuang, Cesium separation from radioactive waste by extraction and adsorption based on crown ethers and calixarenes, *Nucl. Eng. Technol.*, 2020, **52**, 328–336.

5 R. V. d. P. Ferreira, L. G. de Araujo, R. L. S. Canevesi, E. A. da Silva, E. G. A. Ferreira, M. C. Palmieri and J. T. Marumo, The use of rice and coffee husks for biosorption of U (total), ^{241}Am, and ^{137}Cs in radioactive liquid organic waste, *Environ. Sci. Pollut. Res.*, 2020, **27**, 36651–36663.

6 B. Geraldo, L. G. de Araujo, R. Vicente, M. H. T. Taddei, S. M. Cheberle and J. T. Marumo, Radioanalytical methods for sequential analysis of actinide isotopes in activated carbon filter-bed waste, *J. Radioanal. Nucl. Chem.*, 2020, **326**, 1559–1568.

7 C. C. Pavel and K. Popa, Investigations on the ion exchange process of Cs^+ and Sr^{2+} cations by ETS materials, *Chem. Eng. J.*, 2014, **245**, 288–294.

8 USEPA – United States Environmental Protection Agency, *Fact sheet: EPA facts about cesium-137*, 2002, **https://semspub.epa.gov/work/HQ/176309.pdf**, accessed 04 June 2022.

9 J. Wang and C. Chen, Chitosan-based biosorbents: Modification and application for biosorption of heavy metals and radionuclides, *Bioresour. Technol.*, 2014, **160**, 129–141.

10 E. Adams, T. Miyazaki, S. Saito, N. Uozumi and R. Shin, Cesium Inhibits Plant Growth Primarily Through Reduction of Potassium Influx and Accumulation in Arabidopsis, *Plant Cell Physiol.*, 2019, **60**, 63–76.

11 S. Venturi, Cesium in Biology, Pancreatic Cancer, and Controversy in High and Low Radiation Exposure Damage—Scientific, Environmental, Geopolitical, and Economic Aspects, *Int. J. Environ. Res. Public Health*, 2021, **18**, 8934.

12 L. A. Coria-Domínguez, A. Trigos, M. Lizano-Soberón, A. Carrillo-García, I. M. Torres-Víquez, L. A. Medina-Velazquez, A. Esquivel and T. Meza-Menchaca, Synergistic effect in vitro of ergosterol peroxide isolated from *Pleurotus ostreatus* in combination with Cesium – 137 in cervical cancer cell line, *AIP Conf. Proc.*, 2019, **2090**, 020002.

13 S. Yamashita and S. Suzuki, Risk of thyroid cancer after the Fukushima nuclear power plant accident, *Respir. Invest.*, 2013, **51**, 128–133.

14 M. Abtahi, Y. Fakhri, M. Sarafraz, H. Keramati, G. OliveriConti, M. Ferrante, N. Amanidaz, R. Hosseini Pouya, B. Moradi and Z. Baninameh, Removal of cesium through adsorption from aqueous solutions: A systematic review, *J. Adv. Environ. Health Res.*, 2018, **6**, 96–106.

15 J. Wang and S. Zhuang, Removal of cesium ions from aqueous solutions using various separation technologies, *Rev. Environ. Sci. Biotechnol.*, 2019, **18**, 231–269.

16 S. Eun, J. Ryu, H. Kim, H.-J. Hong and S. Kim, Simultaneous removal of radioactive cesium and strontium from seawater using a highly efficient Prussian blue-embedded alginate aerogel, *J. Environ. Manage.*, 2021, **297**, 113389.

17 S. Chen, J. Hu, S. Han, Y. Guo, N. Belzile and T. Deng, A review on emerging composite materials for cesium adsorption and environmental remediation on the latest decade, *Sep. Purif. Technol.*, 2020, **251**, 117340.

18 K. L. M. Taaca and M. R. Vasquez, Fabrication of Ag-exchanged zeolite/chitosan composites and effects of plasma treatment, *Microporous Mesoporous Mater.*, 2017, **241**, 383–391.

19 A. Domard, A perspective on 30 years research on chitin and chitosan, *Carbohydr. Polym.*, 2011, **84**, 696–703.

20 A. K. Singla and M. Chawla, Chitosan: some pharmaceutical and biological aspects - an update, *J. Pharm. Pharmacol.*, 2001, **53**, 1047–1067.

21 J. Wang and S. Zhuang, Chitosan-based materials: Preparation, modification and application, *J. Cleaner Prod.*, 2022, **355**, 131825.

22 M. N. V. Ravi Kumar, A review of chitin and chitosan applications, *React. Funct. Polym.*, 2000, **46**, 1–27.

23 V. K. Thakur and M. K. Thakur, Processing and characterization of natural cellulose fibers/thermoset polymer composites, *Carbohydr. Polym.*, 2014, **109**, 102–117.

24 A. M. Omer, R. Dey, A. S. Eltaweil, E. M. Abd El-Monaem and Z. M. Ziora, Insights into recent advances of chitosan-based adsorbents for sustainable removal of heavy metals and anions, *Arabian J. Chem.*, 2022, **15**, 103543.

25 M. E. Davis, Ordered porous materials for emerging applications, *Nature*, 2002, **417**, 813–821.

26 C. S. Cundy and P. A. Cox, The Hydrothermal Synthesis of Zeolites: History and Development from the Earliest Days to the Present Time, *Chem. Rev.*, 2003, **103**, 663–702.

27 C. S. Cundy and P. A. Cox, The hydrothermal synthesis of zeolites: Precursors, intermediates and reaction mechanism, *Microporous Mesoporous Mater.*, 2005, **82**, 1–78.

28 Z. Shariatinia and A. Bagherpour, Synthesis of zeolite NaY and its nanocomposites with chitosan as adsorbents for lead(II) removal from aqueous solution, *Powder Technol.*, 2018, **338**, 744–763.

29 S. Khandaker, Y. Toyohara, G. C. Saha, M. R. Awual and T. Kuba, Development of synthetic zeolites from bio-slag for cesium adsorption: Kinetic, isotherm and thermodynamic studies, *J. Water Proc. Eng.*, 2020, **33**, 101055.
30 H. Ghobarkar, O. Schäf and U. Guth, Zeolites—from kitchen to space, *Prog. Solid State Chem.*, 1999, **27**, 29–73.
31 L. Pontoni and M. Fabbricino, Use of chitosan and chitosan-derivatives to remove arsenic from aqueous solutions—a mini review, *Carbohydr. Res.*, 2012, **356**, 86–92.
32 L. Roshanfekr Rad and M. Anbia, Zeolite-based composites for the adsorption of toxic matters from water: A review, *J. Environ. Chem. Eng.*, 2021, **9**, 106088.
33 M. V. Dinu and E. S. Dragan, Evaluation of Cu^{2+}, Co^{2+} and Ni^{2+} ions removal from aqueous solution using a novel chitosan/clinoptilolite composite: Kinetics and isotherms, *Chem. Eng. J.*, 2010, **160**, 157–163.
34 D. Humelnicu, M. V. Dinu and E. S. Drăgan, Adsorption characteristics of UO_2^{2+} and Th^{4+} ions from simulated radioactive solutions onto chitosan/clinoptilolite sorbents, *J. Hazard. Mater.*, 2011, **185**, 447–455.
35 J. A. Arcibar-Orozco, A. I. Flores-Rojas, J. R. Rangel-Mendez and P. E. Díaz-Flores, Synergistic effect of zeolite/chitosan in the removal of fluoride from aqueous solution, *Environ. Technol.*, 2020, **41**, 1554–1567.
36 S. Salehi and M. Anbia, Performance comparison of chitosan–clinoptilolite nanocomposites as adsorbents for vanadium in aqueous media, *Cellulose*, 2019, **26**, 5321–5345.
37 T. Watanabe, S. N. Guilhen, J. T. Marumo, R. P. de Souza and L. G. de Araujo, Uranium biosorption by hydroxyapatite and bone meal: evaluation of process variables through experimental design, *Environ. Sci. Pollut. Res.*, 2022, **29**, 79816–79829.
38 E. E. Jasper, J. C. Onwuka and Y. M. Bidam, Screening of factors that influence the preparation of *Dialium guineense* pods active carbon for use in methylene blue adsorption: a full factorial experimental design, *Bull. Natl. Res. Cent.*, 2021, **45**, 168.
39 D. C. Montgomery, *Design and Analysis of Experiments*, John Wiley & Sons, 2017.
40 W. S. W. Ngah, L. C. Teong, C. S. Wong and M. a. K. M. Hanafiah, Preparation and characterization of chitosan–zeolite composites, *J. Appl. Polym. Sci.*, 2012, **125**, 2417–2425.
41 G. E. Box, W. H. Hunter and S. Hunter, *Statistics for Experimenters*, John Wiley and Sons, New York, 1978, vol. 664.
42 *R: The R Project for Statistical Computing*, **https://www.r-project.org/**, accessed 24 February 2022.
43 K. Dunn, *pid: Process Improvement using Data, R package version 0.50*, 2018, **https://CRAN.R-project.org/package=pid**.
44 H. Faghihian, M. Moayed, A. Firooz and M. Iravani, Synthesis of a novel magnetic zeolite nanocomposite for removal of Cs^{+} and Sr^{2+} from aqueous solution: Kinetic, equilibrium, and thermodynamic studies, *J. Colloid Interface Sci.*, 2013, **393**, 445–451.
45 A. Nakamura, K. Sugawara, S. Nakajima and K. Murakami, Adsorption of Cs ions using a temperature-responsive polymer/magnetite/zeolite composite adsorbent and separation of the adsorbent from water using high-gradient magnetic separation, *Colloids Surf., A*, 2017, **527**, 63–69.
46 M. A. Hubbe, S. Azizian and S. Douven, Implications of apparent pseudo-second-order adsorption kinetics onto cellulosic materials: A review, *BioResources*, 2019, **14**, 7582–7626.
47 P. H. Yassue-Cordeiro, C. H. Zandonai, C. F. da Silva, N. R. C. Fernandes-Machado, P. H. Yassue-Cordeiro, C. H. Zandonai, C. F. da Silva and N. R. C. Fernandes-Machado, Desenvolvimento e caracterização de filmes compósitos de quitosana e zeólitas com prata, *Polímeros*, 2015, **25**, 492–502.
48 R. M. Silverstein, F. X. Webster and D. J. Kiemle, *Identificação Espectroscópica de Compostos Orgânicos*, LTC, Rio de Janeiro, 7a edn, 2015.
49 S. Khandaker, M. F. Chowdhury, M. R. Awual, A. Islam and T. Kuba, Efficient cesium encapsulation from contaminated water by cellulosic biomass based activated wood charcoal, *Chemosphere*, 2021, **262**, 127801.
50 M. N. Hasan, M. A. Shenashen, M. M. Hasan, H. Znad and M. R. Awual, Assessing of cesium removal from wastewater using functionalized wood cellulosic adsorbent, *Chemosphere*, 2021, **270**, 128668.
51 O. Eljamal, T. Shubair, A. Tahara, Y. Sugihara and N. Matsunaga, Iron based nanoparticles-zeolite composites for the removal of cesium from aqueous solutions, *J. Mol. Liq.*, 2019, **277**, 613–623.
52 W. S. Wan Ngah, L. C. Teong, R. H. Toh and M. A. K. M. Hanafiah, Comparative study on adsorption and desorption of Cu(II) ions by three types of chitosan–zeolite composites, *Chem. Eng. J.*, 2013, **223**, 231–238.
53 W. S. Wan Ngah, L. C. Teong, R. H. Toh and M. A. K. M. Hanafiah, Utilization of chitosan–zeolite composite in the removal of Cu(II) from aqueous solution: Adsorption, desorption and fixed bed column studies, *Chem. Eng. J.*, 2012, **209**, 46–53.
54 F. Zhang, M. Wang, L. Zhou, X. Ma and Y. Zhou, Removal of Cd(II) from aqueous solution using cross-linked chitosan–zeolite composite, *Desalin. Water Treat.*, 2015, **54**, 2546–2556.
55 A. Gaffer, A. A. Al Kahlawy and D. Aman, Magnetic zeolite-natural polymer composite for adsorption of chromium (VI), *Egypt. J. Pet.*, 2017, **26**, 995–999.
56 M. Pang, N. Kano and H. Imaizumi, Adsorption of chromium (VI) from aqueous solution using zeolite/chitosan hybrid composite, *J. Chem. Chem. Eng.*, 2015, **9**, 433–441.
57 C. Han, T. Yang, H. Liu, L. Yang and Y. Luo, Characterizations and mechanisms for synthesis of chitosan-coated Na–X zeolite from fly ash and As(V) adsorption study, *Environ. Sci. Pollut. Res.*, 2019, **26**, 10106–10116.
58 Y. Zhang, W. Yan, Z. Sun, C. Pan, X. Mi, G. Zhao and J. Gao, Fabrication of porous zeolite/chitosan monoliths and their

applications for drug release and metal ions adsorption, *Carbohydr. Polym.*, 2015, **117**, 657–665.

59 M. M. Motsa, B. B. Mamba, J. M. Thwala and T. A. M. Msagati, Preparation, characterization, and application of polypropylene–clinoptilolite composites for the selective adsorption of lead from aqueous media, *J. Colloid Interface Sci.*, 2011, **359**, 210–219.

60 H. Isawi, Using Zeolite/Polyvinyl alcohol/sodium alginate nanocomposite beads for removal of some heavy metals from wastewater, *Arabian J. Chem.*, 2020, **13**, 5691–5716.

61 V. Litrenta Medeiros, L. G. de Araujo, D. Rubinho Ratero, A. Silva Paula, E. Ferreira Molina, C. Jaeger, J. T. Marumo and J. G. Nery, Synthesis and physicochemical characterization of a novel adsorbent based on yttrium silicate: A potential material for removal of lead and cadmium from aqueous media, *J. Environ. Chem. Eng.*, 2020, **8**, 103922.

62 J. Wang and X. Guo, Adsorption kinetic models: Physical meanings, applications, and solving methods, *J. Hazard. Mater.*, 2020, **390**, 122156.

63 E. H. Borai, R. Harjula, L. Malinen and A. Paajanen, Efficient removal of cesium from low-level radioactive liquid waste using natural and impregnated zeolite minerals, *J. Hazard. Mater.*, 2009, **172**, 416–422.

64 K. Wang, H. Ma, S. Pu, C. Yan, M. Wang, J. Yu, X. Wang, W. Chu and A. Zinchenko, Hybrid porous magnetic bentonite-chitosan beads for selective removal of radioactive cesium in water, *J. Hazard. Mater.*, 2019, **362**, 160–169.

65 R. V. P. Ferreira, E. A. Silva, R. L. S. Canevesi, E. G. A. Ferreira, M. H. T. Taddei, M. C. Palmieri, F. R. O. Silva and J. T. Marumo, Application of the coconut fiber in radioactive liquid waste treatment, *Int. J. Environ. Sci. Technol.*, 2018, **15**, 1629–1640.

66 L. C. Vieira, L. G. de Araujo, R. V. de Padua Ferreira, E. A. da Silva, R. L. S. Canevesi and J. T. Marumo, Uranium biosorption by *Lemna* sp. and *Pistia stratiotes*, *J. Environ. Radioact.*, 2019, **203**, 179–186.

67 L. G. de Araujo, L. C. Vieira, R. L. S. Canevesi, E. A. da Silva, T. Watanabe, R. V. de Padua Ferreira and J. T. Marumo, Biosorption of uranium from aqueous solutions by *Azolla* sp. and *Limnobium laevigatum*, *Environ. Sci. Pollut. Res.*, 2022, **29**, 45221–45229.

68 A. F. T. El-Din, E. A. Elshehy, M. O. A. El-Magied, A. A. Atia and M. E. El-Khouly, Decontamination of radioactive cesium ions using ordered mesoporous monetite, *RSC Adv.*, 2018, **8**, 19041–19050.